The Aeronautical Journal (2022), **126**, pp. 1026–1044
doi:10.1017/aer.2021.117

REGULAR PAPER

Cooperative guidance law for intercepting a hypersonic target with impact angle constraint

S. Liu[1], B. Yan[2], R. Liu[2], P. Dai[2], J. Yan[1] and G. Xin[3]

[1]Unmanned System Research Institute, Northwestern Polytechnical University, Xi'an 710072, China, [2]School of Astronautics, Northwestern Polytechnical University, Xi'an 710072, China and [3]Aerospace System Engineering Shanghai, Shanghai 201100, China
E-mail: yanbinbin@nwpu.edu.cn

Received: 6 June 2021; **Revised:** 11 October 2021; **Accepted:** 25 November 2021

Keywords: Cooperative guidance; Consensus theory; Super-twisting algorithm; Hypersonic targets

Abstract

The cooperative guidance problem of multiple inferior missiles intercepting a hypersonic target with the specific impact angle constraint in the two-dimensional plane is addressed in this paper, taking into consideration variations in a missile's speed. The guidance law is designed with two subsystems: the direction of line-of-sight (LOS) and the direction of normal to LOS. In the direction of LOS, by applying the algebraic graph theory and the consensus theory, the guidance command is designed to make the system convergent in a finite time to satisfy the goal of cooperative interception. In the direction of normal to LOS, the impact angle is constrained to transform into the LOS angle at the time of interception. In view of the difficulty of measuring unknown target acceleration information in real scenarios, the guidance command is designed by utilising a super-twisting algorithm based on a nonsingular fast-terminal sliding mode (NFTSM) surface. Numerical simulation results manifest that the proposed guidance law performs efficiently and the guidance commands are free of chattering. In addition, the overall performance of this guidance law is assessed with Monte Carlo runs in the presence of measurement errors. The simulation results demonstrate that the robustness can be guaranteed, and that overall efficiency and accuracy in intercepting the hypersonic target are achieved.

Nomenclature

OXY	inertial coordinate system
M_i	missile i
T	hypersonic target
R_i	relative range between the missile i and the hypersonic target
V_i	speed of the missile i
V_T	speed of the hypersonic target
γ_i	LOS angle of the missile i
θ_i	flight path angle of the missile i
θ_T	flight path angle of the hypersonic target
η_i	heading angle of the missile i
η_T	heading angle of the hypersonic target
a_i	normal acceleration of the missile i
a_T	normal acceleration of the hypersonic target

1.0 Introduction

Hypersonic flight technology, a highlight of the 21st-century aviation and aerospace industries, has enabled hypersonic vehicles to reach speed of over Mach 5 [1], with far-reaching military and economic

implications; for example, a dramatic increase in penetration rate [2]. In contrast to targets moving outside the atmosphere or in the dense atmosphere, hypersonic targets flying in near space have long-time continuous manoeuvering trajectories rather than ballistic fixed trajectories. In addition, the combination of hypersonic flight technology, trajectory planning methods and morphing technology can prepare hypersonic aircrafts to complete complex missions in more challenging combat environments, which subverts existing strike methods and traditional defense systems, and greatly expands the combat space [3–7]. The unconventional ballistic flight characteristics and manoeuver ability of hypersonic vehicles make it difficult to intercept them efficiently with single missile by traditional guidance laws [1, 8]. A more advanced strategy of deploying multiple missiles to intercept hypersonic vehicles is therefore more likely to be effective.

Multiple missiles can work together to improve the effectiveness of a defense system against single missile in the context of a shared and complementary information network. An important advantage of a multiple-missile system is the capability to share combat information, leading to improvement in target penetration: Even if several missiles are intercepted, the target can still be destroyed by the remaining missiles [9]. As a result, when multiple missiles attack cooperatively, the interception efficiency of the specific target and the penetration capability of missiles will be extensively improved. The design of multi-missile system cooperative guidance laws is one of the key technologies that enable multiple missiles to accurately intercept large manoeuvering targets [10, 11].

Cooperative guidance for intercepting targets has been studied extensively in recent years, with two principal methods emerging as the forerunners in the field. With the first method, the interception time for each missile needs to be determined in advance, which requires calculation of the remaining interception time to be very precise. In [12], a biased proportional navigation guidance law was constructed in which the actual interception time was derived analytically by solving the system differential equations. In [13], based on a leader-follower cooperative salvo guidance strategy, an improved estimate of time-to-go, that did not assume a small heading angle of the interceptor, was used in the guidance design. Relying on the estimation of remaining interception time, the multi-missiles cooperative interception problem with communication delay was investigated in [14]. In [15], a modified cooperative guidance law was presented to avoid singularities existing in the guidance law on the basis of the estimation of remaining interception time. Also, based on the fundamentals of the above research, other groups took the impact angle control guidance (IACG) into consideration to improve interception effectiveness on targets [12, 16].

The second method was developed from the concept of multi-agent consensus protocol: multiple missiles attack the target simultaneously by establishing a communication network. In [17], a new guidance scenario was investigated, involving impact time constraint: a feedback loop of the impact time error was combined with the traditional optimal feedback loop to reduce miss distance and minimise control effort, enabling in-flight control of the impact time. Ref [18] addressed a distributed cooperative guidance law by using the relative distance between missile and target as well as lead angle as coordination variables. However, this strategy is only suitable for stationary targets and not accurate for high-speed manoeuvering targets. In [19], based on the undirected graph theory, a new finite-time consensus protocol for the LOS direction was derived to guarantee the goal of cooperative attack. Ref [20] proposed a cooperative guidance law based on consensus theory, intended for multiple missiles against a manoeuvering target in the three-dimensional plane. Moreover, an expected impact angle should be taken into consideration in the course of a cooperative intercept mission in order to improve the lethality and interception rate of missiles. A novel cooperative guidance law with impact angle constraints, based on multi-agent consensus theory, was proposed in [21–23]. However, these methods are only suitable for stationary or low-speed manoeuvering targets, which are unrepresentative of actual combat scenarios.

The two methods mentioned were established under the assumption that the speed of the missile was a constant. In many practical situations, however, this assumption is restrictive and idealistic. Thus, it is important to take variations of missile speed into account. In [24], an impact time control guidance (ITCG) law for cooperative attack was proposed in which only the variation range of the missile speed needs to be considered, a relaxation of the constant speed assumption. In [25], the authors developed

https://doi.org/10.1017/aer.2021.117 Published online by Cambridge University Press

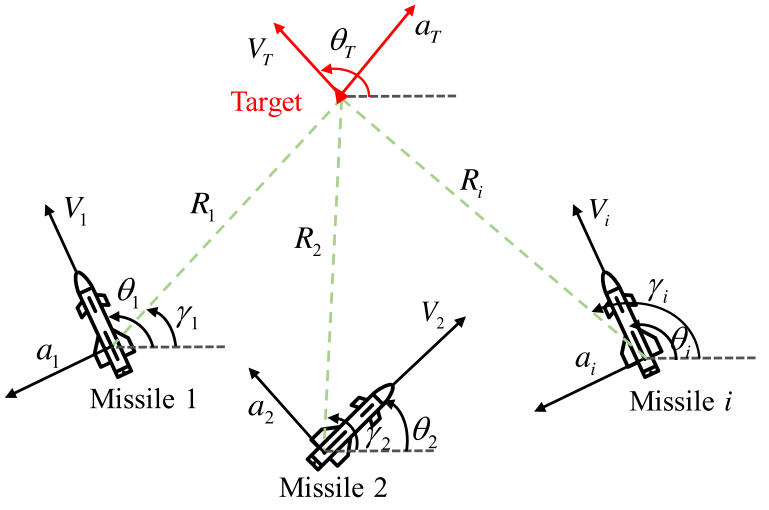

Figure 1. *Geometry of cooperative guidance.*

a novel ITCG law for guided projectiles considering time-varying speed, which could satisfy the constraints of both miss distance and impact time. In addition, in view of the external disturbances connected to the manoeuvering of the target in [20, 22], a non-homogeneous disturbance observer was designed to estimate the external disturbance.

Based on the above research, this paper presents a cooperative guidance scheme for multiple inferior missiles intercepting a hypersonic target with impact angle constraint. The main contributions of this paper can be summarised as follows:

(1) In the process of guidance design, varying missile speed is taken into consideration in order to improve the manoeuverability and combat effectiveness of missiles.

(2) For unknown external disturbances arising from manoeuvering of the target, the super-twisting algorithm is adopted to obviate the requirement for estimating the external disturbances.

(3) The constraint of impact angle at interception is considered so as to promote target damage efficiency and implement a multi-directional interception mode.

The remainder of this paper is organised as follows: Section 2 addresses the problem of missiles intercepting a hypersonic target in the two-dimensional plane; the design of the guidance commands is outlined in sections 3 and 4; comparative simulation studies are presented in section 5; and conclusions are drawn in section 6.

2.0 Problem statement

For the convenience of modeling and analysis, it is assumed that multiple inferior missiles intercept a hypersonic target cooperatively in the two-dimensional plane, as in Fig. 1. The relative motion model between a missile $i, i \in (1, 2, \cdots, n) n \in \mathbb{R}^+$ and its target is expressed as follows:

$$\dot{R}_i = V_T \cos \eta_T - V_i \cos \eta_i \tag{1}$$

$$R_i \dot{\gamma}_i = V_i \sin \eta_i - V_T \sin \eta_T \tag{2}$$

$$\eta_i = \gamma_i - \theta_i \tag{3}$$

$$\eta_T = \gamma_i - \theta_T \tag{4}$$

https://doi.org/10.1017/aer.2021.117 Published online by Cambridge University Press

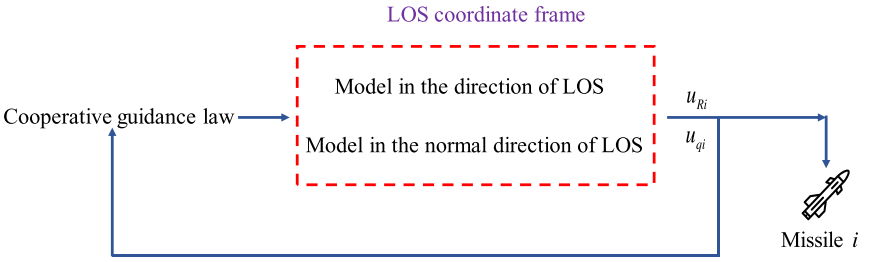

Figure 2. *Cooperative guidance law scheme.*

$$\dot{\theta}_i = a_i / V_i \tag{5}$$

$$\dot{\theta}_T = a_T / V_T \tag{6}$$

One then takes the derivative of Equations (1)-(2)

$$\ddot{R}_i = \omega_{Ri} - u_{Ri} + R_i \dot{\gamma}_i^2 \tag{7}$$

$$\ddot{\gamma}_i = -\frac{2\dot{R}_i \dot{\gamma}_i}{R_i} + \frac{\omega_{qi}}{R_i} - \frac{u_{qi}}{R_i} \tag{8}$$

where u_{Ri} and u_{qi} are two components of the normal acceleration a_i, respectively. $u_{Ri} = a_i \cos \eta_i + a_i \sin \eta_i$ represents the part of a_i along LOS, and $u_{qi} = a_i \sin \eta_i - a_i \cos \eta_i$ is the part of a_i normal to LOS. ω_{Ri} and ω_{qi} are two components of the normal acceleration a_T, respectively. $\omega_{Ri} = a_T \cos \eta_T + a_T \sin \eta_T$ represents the part of a_T along LOS, and $\omega_{qi} = a_T \cos \eta_T - a_T \sin \eta_T$ is the part of a_T normal to LOS. Usually, ω_{Ri} and ω_{qi} cannot be measured directly, and thus they are regarded as external disturbances.

The core of a successful cooperative interception process for multiple missiles is that missiles intercept the target simultaneously, accurately and effectively, which means that multiple missiles need to satisfy the constraints of both time convergence and interception accuracy. In addition, in order to improve damage efficiency on the target, IACG should be taken into consideration. Generally, the impact angle constraint translates into controlling the LOS angle at interception [16, 26]. Thus, the design objectives of cooperative guidance law for the purposes of this paper can be described as follows:

$$\begin{cases} \lim_{t \to t_f} R_i = 0 \\ \lim_{t \to t_f} \gamma_i = \gamma_i^d \\ \lim_{t \to t_f} \dot{\gamma}_i = 0 \\ t_f^1 = t_f^2 = \cdots = t_f^i \end{cases} \tag{9}$$

where t_f^i is the total interception time of the missile i. γ_i^d represents the desired impact angle of the missile i.

Letting $x_{1i} = R_i, x_{2i} = \dot{R}_i, x_{3i} = \gamma_i - \gamma_i^d, x_{4i} = \dot{\gamma}_i$, then based on Equations (1)-(8), the cooperative guidance system model can be expressed as

$$\begin{cases} \dot{x}_{1i} = x_{2i} \\ \dot{x}_{2i} = x_{1i} x_{4i}^2 - u_{Ri} + \omega_{Ri} \\ \dot{x}_{3i} = x_{4i} \\ \dot{x}_{4i} = -\dfrac{2x_{2i}x_{4i}}{x_{1i}} - \dfrac{u_{qi}}{x_{1i}} + \dfrac{\omega_{qi}}{x_{1i}} \end{cases} \tag{10}$$

As shown in Equation (10), there are coupling characteristics in the model. However, since the acceleration commands u_{Ri} and u_{qi} are separated, coupling characteristics can be eliminated through feedback decoupling control. Figure 2 reveals that the cooperative guidance scheme can be divided into two

https://doi.org/10.1017/aer.2021.117 Published online by Cambridge University Press

channels, including the LOS direction and LOS normal direction. By designing guidance commands u_{Ri} and u_{qi} independently, multiple missiles can be organised to intercept a target accurately, with the impact angle simultaneously constraint.

3.0 Guidance command design along LOS

Before designing the guidance law to achieve the goal of intercepting a target accurately and effectively with multiple missiles, some preliminary assumptions need to be put forward:

Assumption 1. *All missiles and the target are treated as ideal mass points, ignoring their shape.*

Assumption 2. *The influence of the rotation of the earth and the external environment on the missiles and the target can be ignored.*

3.1 Algebraic graph theory

In this subsection, we introduce the concept of algebraic graph theory, which was put forward in [27, 28]. Supposing that a team of agents interact with each other through a communication or sensing network or a combination of both; it is natural to model the interaction among agents with graphs. A graph in this paper is a diagram composed of nodes and edges (also called links or lines), which respectively represent objects and their connections.

A graph $G =< N(G), E(G), \varphi(G) >$ is composed of multiple nodes and edges connecting nodes. $N(G) = \{n_1, n_2, \cdots, n_n\}$ $(N(G) \neq \emptyset)$ denotes the vertex set (the nodes) of graph G, where $n_i (i = 1, 2, \cdots, n)$ represents a single agent. $E(G) = \{e_1, e_2, \cdots e_m\}$ denotes the edge set where $e_i = \left\{ (n_i, n_j) \,\middle|\, i \neq j, n_i, n_j \in V \right\}$ $(i = 1, 2, \cdots, n)$ represents the connection and communication between agents n_i and n_j. $\varphi(G)$ denotes the incidence function, which indicates the correspondence between n_i and e_i.

There are two main types of graphs: directed and undirected. In a directed graph, a cycle is a directed path that starts and ends at the same node. A directed graph is strongly connected if there is a directed path from every node to every other node. An undirected graph is strongly connected if there is an undirected path between every pair of distinct nodes. Note that $A = \left(a_{ij}\right)_{n \times n} \left(a_{ij} \geq 0, i \neq j\right)$ represents the adjacency matrix of a given graph. For an undirected graph, when missile i can receive information from missile j, a_{ij}=1. Otherwise, a_{ij}=0.

Assumption 3. *A communication network composed of multiple missiles can be regarded as a multi-agent system with mutual communication represented by edges. The topology of this information interaction can be described by a graph.*

Assumption 4. *In this paper, the graph G made up of multiple missiles is regarded as undirected and connected and the communication between them is ideal.*

3.2 Guidance command design

Before designing the guidance command u_{Ri}, we will begin with some definitions and lemmas:

Definition 1. [29] *Subject to the following multi-agent system*

$$\begin{cases} \dot{\xi}_i = v_i \\ \dot{v}_i = u_i \end{cases} \tag{11}$$

where $\xi_i, v_i, u_i \in \mathbb{R}$ represent the position, speed and acceleration information of the i-th agent, respectively. Especially u_i stands for the second-order consistency algorithm if the proposed u_i can ensure that ξ_i and v_i converge at instant T.

https://doi.org/10.1017/aer.2021.117 Published online by Cambridge University Press

Definition 2. [30] *For the following system*

$$\dot{\boldsymbol{x}} = \boldsymbol{f}(\boldsymbol{x}, t), \boldsymbol{f}(\boldsymbol{0}, t) = \boldsymbol{0}, \boldsymbol{x} \in \mathbb{R}^n \tag{12}$$

with $\boldsymbol{x} \in U \subseteq \mathbb{R}^n$*, continuous on an open neighborhood* U *of the origin. Supposing that for arbitrary initial condition* $\boldsymbol{x}(\boldsymbol{0}) = \boldsymbol{x}_0 \in U_0 \subseteq U$*, Equation (13) can be established when* $T > 0$*.*

$$\begin{cases} \lim\limits_{t \to T(x_0)} \boldsymbol{x}(t, \boldsymbol{0}, \boldsymbol{x}_0) = \boldsymbol{0} \\ \boldsymbol{x}(t, \boldsymbol{0}, \boldsymbol{x}_0) = \boldsymbol{0}, t > T(\boldsymbol{x}_0) \end{cases} \tag{13}$$

Then, $\boldsymbol{x}$ will converge to be the origin $\boldsymbol{x} = \boldsymbol{0}$ in a finite time. If the origin is Lyapunov stable and finite-time convergent in a neighbourhood of the origin, $\boldsymbol{x} = \boldsymbol{0}$ is stable for a finite time. When $U = \mathbb{R}^n$, $\boldsymbol{x} = \boldsymbol{0}$ is globally stable for a finite time.

Lemma 1. [31] *Assume that* $\boldsymbol{x}(t)$ *is the solution of* $\dot{\boldsymbol{x}} = \boldsymbol{f}(\boldsymbol{x}, t)$ *and* $\boldsymbol{x}(0) = \boldsymbol{x}_0 \in \mathbb{R}^n$*, where* $\boldsymbol{f}$ *denotes* $\boldsymbol{U} \to \mathbb{R}^n$ *is continuous with* $\boldsymbol{U}$ *an open subset of* $\mathbb{R}^n$*. Setting* $V: \boldsymbol{U} \to \mathbb{R}$ *is a locally Lipschitz function and satisfies* $D^+V(\boldsymbol{x}(t)) \leq 0$*, where* D^+ *represents the upper Dini derivative. Then noting the positive set as* $\Lambda^+(\boldsymbol{x}_0)$*,* $\Lambda^+(\boldsymbol{x}_0) \cap U$ *is contained in the union of* $\boldsymbol{S} = \{\boldsymbol{x} \in \boldsymbol{U} | D^+V(\boldsymbol{x}) = 0\}$*.*

Lemma 2. [32] *The system (12) can be regarded as homogeneous if the following formula holds for arbitrary* $\varepsilon > 0$*.*

$$f_i\left(\varepsilon^{\delta_1} x_1, \varepsilon^{\delta_2} x_2, \ldots, \varepsilon^{\delta_n} x_n\right) = \varepsilon^{\sigma + \delta_i} f_i(\boldsymbol{x}), \quad i = 1, 2, \ldots, n \tag{14}$$

where $\delta_i, \sigma \in \mathbb{R}$ *and* σ *is the homogeneity degree of the system (12).*

Lemma 3. [33] *If the system (12) is asymptotically stable and homogeneous, with the homogeneity degree* $\sigma < 0$*, then the system (12) is finite-time stable.*

Generally, in the process of terminal guidance law design, only the acceleration command normal to LOS is taken into account in order to attack the target accurately, while the normal acceleration instruction in the direction of LOS is ignored. Actually, since guidance time is not infinite for each missile, it is essential to consider the guidance command in the direction of LOS.

Based on the system (10), the cooperative guidance model in the direction of LOS can be described as

$$\begin{cases} \dot{x}_{1i} = x_{2i} \\ \dot{x}_{2i} = x_{1i} x_{4i}^2 - u_{Ri} + \omega_{Ri} \end{cases} \tag{15}$$

Generally, the target is manoeuvering in the direction of normal to LOS. Thus, the component of the target acceleration $\omega_{Ri} = 0$ holds. As a result, Equation (15) can be transformed into the following form

$$\begin{cases} \dot{x}_{1i} = x_{2i} \\ \dot{x}_{2i} = x_{1i} x_{4i}^2 - u_{Ri} \end{cases} \tag{16}$$

Theorem 1. *Subject to the system (16), based on the protocol of consensus theory,* x_{1i} *and* x_{2i} *will converge in a finite time with the appropriate choice of parameters under the action of guidance command* u_{Ri}*.*

$$u_{Ri} = x_{1i} x_{4i}^2 + \sum_{j=1}^{n} a_{ij} \left[q_{1i} \left(sig\left(x_{1i} - x_{1j}\right)^{\alpha_1} \right) + q_{2i} \left(sig\left(x_{2i} - x_{2j}\right)^{\alpha_2} \left| x_{1i} - x_{1j} \right|^{\alpha_3} \right) \right] \tag{17}$$

where $0 < \alpha_i < 1, (i = 1, 2, 3)$ *with* $2(\alpha_1 - \alpha_3) = (1 + \alpha_1)\alpha_2$ *and* $sig(\bullet)^{\alpha} = |\bullet|^{\alpha} \operatorname{sgn}(\bullet)$*.* a_{ij} *is the element of the adjacency matrix of graph G.* q_{1i} *and* q_{2i} *are positive parameters that need to be designed.*

https://doi.org/10.1017/aer.2021.117 Published online by Cambridge University Press

Proof. Substituting Equation (17) into Equation (16), yields

$$\begin{cases} \dot{x}_{1i} = x_{2i} \\ \dot{x}_{2i} = -\sum_{j=1}^{n} a_{ij}\left[q_{1i}\left(sig\left(x_{1i}-x_{1j}\right)^{\alpha_1}\right)+q_{2i}\left(sig\left(x_{2i}-x_{2j}\right)^{\alpha_2}\left|x_{1i}-x_{1j}\right|^{\alpha_3}\right)\right] \end{cases} \tag{18}$$

Since the graph G is undirected, $a_{ij} = a_{ji}$ holds. Then, for $t \geq 0$, we can obtain that

$$\sum_{i=1}^{n} \dot{x}_{2i} \equiv 0 \tag{19}$$

Taking a Lyapunov function V_1

$$V_1 = \sum_{i=1}^{n}\sum_{j=1}^{n}\int_0^{x_{1i}-x_{1j}} a_{ij}q_{1i}(sig(s)^{\alpha_1})\,ds + \frac{1}{2}\sum_{i=1}^{n} x_{2i}^2 \tag{20}$$

Note that $sig(\bullet)^{\alpha}$ is an odd function. For Equation (20), it is positive-definite with respect to $x_{1i} - x_{1j}$, $(\forall i \neq j)$ and x_{2i}, $(\forall i \in I_n)$. Considering the derivative of V_1 with respect t, leads to

$$\begin{aligned} \dot{V}_1 &= \sum_{i=1}^{n}\sum_{j=1}^{n} a_{ij}q_{1i}\left(sig\left(x_{1i}-x_{1j}\right)^{a_1}\right)x_{2i} + \sum_{i=1}^{n} x_{2i}\dot{x}_{2i} \\ &= \sum_{i=1}^{n}\sum_{j=1}^{n} a_{ij}q_{1i}\left(sig\left(x_{1i}-x_{1j}\right)^{a_1}\right)x_{2i} - \sum_{i=1}^{n}\sum_{j=1}^{n} x_{2i}a_{ij}\left[q_{1i}\left(sig\left(x_{1i}-x_{1j}\right)^{\alpha_1}\right)\right. \\ &\quad \left. + q_{2i}\left(sig\left(x_{2i}-x_{2j}\right)^{\alpha_2}\left|x_{2i}-x_{2j}\right|^{\alpha_3}\right)\right] \\ &= -q_{2i}\sum_{i=1}^{n}\sum_{j=1}^{n} x_{2i}a_{ij}\left(sig\left(x_{2i}-x_{2j}\right)^{\alpha_2}\left|x_{2i}-x_{2j}\right|^{\alpha_3}\right) \\ &= -\frac{1}{2}q_{2i}\sum_{i=1}^{n}\sum_{j=1}^{n}\left(x_{2i}-x_{2j}\right)a_{ij}\left(sig\left(x_{2i}-x_{2j}\right)^{\alpha_2}\left|x_{2i}-x_{2j}\right|^{\alpha_3}\right) \\ &= -\frac{1}{2}q_{2i}\sum_{i=1}^{n}\sum_{j=1}^{n} a_{ij}\left|x_{2i}-x_{2j}\right|^{1+\alpha_2+\alpha_3} \\ &\leq 0 \end{aligned} \tag{21}$$

Setting $\dot{V}_1 = 0$, we get

$$x_{2i} = x_{2j} \tag{22}$$

Then, based on Equation (18) and Equation (22), one can obtain

$$\dot{x}_{2i} = -\sum_{j=1}^{n} a_{ij}q_{1i}\mathrm{sig}\left(x_{1i}-x_{1j}\right)^{\alpha_1} \tag{23}$$

And taking the derivative of Equation (22)

$$\dot{x}_{2i} = \dot{x}_{2j} \tag{24}$$

On the basis of Equation (19) and Equation (24), we get

$$\dot{x}_{2i} = 0 \tag{25}$$

Substituting Equation (25) into Equation (23), reveals that

$$\sum_{j=1}^{n} a_{ij}q_{1i}\mathrm{sig}\left(x_{1i}-x_{1j}\right)^{\alpha_1} = 0 \tag{26}$$

https://doi.org/10.1017/aer.2021.117 Published online by Cambridge University Press

Thus, Equation (27) can be established as

$$q_{1i}\sum_{i=1}^{n}x_{1i}\sum_{j=1}^{n}a_{ij}\mathrm{sig}\left(x_{1i}-x_{1j}\right)^{\alpha_1}=0 \tag{27}$$

On the other hand

$$\begin{aligned}q_{1i}\sum_{i=1}^{n}x_{1i}\sum_{j=1}^{n}a_{ij}\mathrm{sig}\left(x_{1i}-x_{1j}\right)^{\alpha_1}&=\frac{1}{2}q_{1i}\sum_{i=1}^{n}\sum_{j=1}^{n}a_{ij}\left(x_{1i}-x_{1j}\right)\mathrm{sig}\left(x_{1i}-x_{1j}\right)^{\alpha_1}\\&=\frac{1}{2}q_{1i}\sum_{i=1}^{n}\sum_{j=1}^{n}a_{ij}\left|x_{1i}-x_{1j}\right|^{1+\alpha_1}\end{aligned} \tag{28}$$

Combined with Equations (27)-(28), it can be conducted that

$$\frac{1}{2}q_{1i}\sum_{i=1}^{n}\sum_{j=1}^{n}a_{ij}\left|x_{1i}-x_{1j}\right|^{1+\alpha_1}=0 \tag{29}$$

Since the graph G is undirected and connected

$$x_{1i}=x_{1j} \tag{30}$$

As a consequence, based on Equation (22) and Equation (25), when $\dot{V}_1=0$, $x_{2i}=c_1, c_1\in\mathbb{R}$ holds. Thus, $x_{1i}=c_1t+c_2, c_2\in\mathbb{R}$ holds.

Therefore, relying on lemma 1, results in

$$\lim_{t\to\infty}x_{1i}=c_1t+c_2,\ \lim_{t\to\infty}x_{2i}=c_1 \tag{31}$$

Defining two intermediate variables $\tilde{x}_{1i}$ and $\tilde{x}_{2i}$

$$\begin{cases}\tilde{x}_{1i}=x_{1i}-(c_1t+c_2)\\ \tilde{x}_{2i}=x_{2i}-c_1\end{cases} \tag{32}$$

Then, based on Equations (31)-(32), one can see that

$$\lim_{t\to\infty}\tilde{x}_{1i}=0,\ \lim_{t\to\infty}\tilde{x}_{2i}=0 \tag{33}$$

On the basis of Equation (32), the system (18) can be converted as follows:

$$\begin{cases}\dot{\tilde{x}}_{1i}=\tilde{x}_{2i}\\ \dot{\tilde{x}}_{2i}=-\sum_{j=1}^{n}a_{ij}\left[q_{1i}\mathrm{sig}\left(\tilde{x}_{1i}-\tilde{x}_{1j}\right)^{\alpha_1}+q_{2i}\left(sig\left(\tilde{x}_{2i}-\tilde{x}_{2j}\right)^{\alpha_2}\left|\tilde{x}_{2i}-\tilde{x}_{2j}\right|^{\alpha_3}\right)\right]\end{cases} \tag{34}$$

Next, according to Equation (33) and lemma 3, it is essential to prove that the system (34) is homogeneous with the homogeneity degree $\sigma<0$ so as to demonstrate that $\tilde{x}_{1i}$ and $\tilde{x}_{2i}$ can converge in a finite time.

After, defining a new variable $\boldsymbol{\zeta}=(\tilde{x}_{11},\tilde{x}_{12},...,\tilde{x}_{1n},\tilde{x}_{21},\tilde{x}_{22},...,\tilde{x}_{2n})^T\in\mathbb{R}^{2n}$, the system (34) can be equivalent to $\dot{\boldsymbol{\zeta}}=f(\boldsymbol{\zeta})$. Based on lemma 2, one can obtain

$$f_i\left(\varepsilon^{\delta_1}\hat{x}_{11},\ldots,\varepsilon^{\delta_n}\hat{x}_{1n},\varepsilon^{\delta_{n+1}}\hat{x}_{21},\ldots,\varepsilon^{\delta_{2n}}\hat{x}_{2n}\right)=\varepsilon^{\delta_{m+i}}\hat{x}_{2i}=\varepsilon^{K+\delta_i}\hat{x}_{2i} \tag{35}$$

$$\begin{aligned}&f_{n+i}\left(\varepsilon^{\delta_1}\hat{x}_{11},\ldots,\varepsilon^{\delta_n}\hat{x}_{1n},\varepsilon^{\delta_{m+1}}\hat{x}_{21},\ldots,\varepsilon^{\delta_{2n}}\hat{x}_{2n}\right)\\&=-\sum_{j=1}^{n}a_{ij}\left[q_{1i}\mathrm{sig}\left(\tilde{x}_{1i}-\tilde{x}_{1j}\right)^{\alpha_1}+q_{2i}\left(sig\left(\tilde{x}_{2i}-\tilde{x}_{2j}\right)^{\alpha_2}\left|\tilde{x}_{2i}-\tilde{x}_{2j}\right|^{\alpha_3}\right)\right]\\&=-\varepsilon^{K+\delta_{n+1}}\sum_{j=1}^{n}a_{ij}\left[q_{1i}\mathrm{sig}\left(\tilde{x}_{1i}-\tilde{x}_{1j}\right)^{\alpha_1}+q_{2i}\left(sig\left(\tilde{x}_{2i}-\tilde{x}_{2j}\right)^{\alpha_2}\left|\tilde{x}_{2i}-\tilde{x}_{2j}\right|^{\alpha_3}\right)\right]\end{aligned} \tag{36}$$

https://doi.org/10.1017/aer.2021.117 Published online by Cambridge University Press

According to Equations (35)-(36), we get

$$\begin{cases} \delta_{n+i} = \sigma_1 + \delta_i \\ \delta_i = \delta_j \\ \delta_i \alpha_1 = \sigma_1 + \delta_{n+i} \end{cases} \tag{37}$$

Setting $\delta_i = 2$, the homogeneity degree of the system (34) is $\sigma_1 = \alpha_1 - 1 < 0$, revealing in the system (34) is homogeneous. Thus, by applying lemma 3, one obtains

$$\lim_{t \to T_1} \tilde{x}_{1i} = 0, \lim_{t \to T_1} \tilde{x}_{2i} = 0, T_1 > 0 \tag{38}$$

Substituting Equation (32) into Equation (38), gives

$$\lim_{t \to T_1} x_{1i} = c_1 t + c_2, \lim_{t \to T_1} x_{2i} = c_1, T_1 > 0 \tag{39}$$

Consequently, Equation (39) demonstrates that x_{1i} and x_{2i} will converge in a finite time under the action of the proposed guidance command u_{Ri}, which shows that in the direction of LOS, u_{Ri} can adjust the value of R_i and $\dot{R}_i$ to be consistent in a finite time to achieve the time convergence based on the consensus theory. Thus, theorem 1 has been proven completely.

4.0 Guidance command design for normal to LOS

In this subsection, we design guidance command in the direction of normal to LOS, to guarantee IACG that will to improve target damage efficiency. Based on the system (10), the cooperative guidance system model for the direction of normal to LOS can be obtained as follows:

$$\begin{cases} \dot{x}_{3i} = x_{4i} \\ \dot{x}_{4i} = -\dfrac{2x_{2i}x_{4i}}{x_{1i}} - \dfrac{u_{qi}}{x_{1i}} + \dfrac{\omega_{qi}}{x_{1i}} \end{cases} \tag{40}$$

Assumption 5. *The component $d_{qi} = \omega_{qi}/x_{1i}$ is regarded as the external disturbance with the upper boundary D_i caused by the manoeuverability of the target. It is cannot be measured during the interception process.*

For the system (40), which is inspired by Ref [34], a type of nonsingular fast terminal sliding mode (NFTSM) surface is applied to design the sliding mode variable S_i to ensure the finite-time convergence of x_{3i} and x_{4i}.

$$S_i = x_{4i} + \beta_{1i} x_{3i} + \beta_{2i} e^{-\lambda_i t} \left(x_{3i}^T x_{3i} \right)^{-h_i} x_{3i} \tag{41}$$

where e is the base of natural logarithm. β_{1i}, β_{2i}, λ_i and h_i are all the positive parameters remaining to be designed.

In order to suppress external disturbance and reduce the chattering phenomenon of the guidance command, by employing the NFTSM sliding mode surface, we designed the guidance command for the direction of normal to LOS based on the super-twisting algorithm. Using this method, we can stabilise both the states of the perturbed double-integrator asymptotically using continuous control, which is good from a practical point of view [35, 36].

Lemma 4. [37]. *For a nonlinear system $\dot{\boldsymbol{x}} = f(\boldsymbol{x})\boldsymbol{x} \in \mathbb{R}^n$ with $f(0) = 0$. $\boldsymbol{U}^0 \subset \mathbb{R}^n$ is defined within an open neighborhood of the origin. One must choose $V(\boldsymbol{x})$ to be positive definite, which is true for all states in the open neighborhood $\boldsymbol{U}^0$. There is a positive constant m. Then the following inequality can be established*

$$\dot{V}(\boldsymbol{x}) + mV(\boldsymbol{x})^n \leq 0 \quad n \in (0, 1) \tag{42}$$

As a result, the equilibrium point of the system converges in a finite time.

https://doi.org/10.1017/aer.2021.117 Published online by Cambridge University Press

Theorem 2. *In the presence of assumption 5, and governed by the guidance command in Equation (43), all state variables existing in the system (40) will converge to zero in a finite time. That is, both* $\lim_{t\to t_f}\gamma_i=\gamma_i^d$ *and* $\lim_{t\to t_f}\dot{\gamma}_i=0$ *can be satisfied in a finite time.*

$$u_{qi}=u_{eqi}+u_{STWi} \tag{43}$$

where

$$\begin{cases} u_{eqi}=-b_i(x)^{-1}\left(-\dfrac{2x_{2i}x_{4i}}{x_{1i}}+\beta_{1i}x_{4i}+\beta_{2i}A_i\right) \\ u_{STWi}=-b_i(x)^{-1}\left(k_{1i}|S_i|^{1/2}sign\,(S_i)+z_i\right) \\ \dot{z}_i=-k_{2i}sign\,(S_i) \end{cases} \tag{44}$$

$$A_i=(-\lambda_i)\,e^{-\lambda_i t}\left(x_{3i}^Tx_{3i}\right)^{-h_i}x_3-e^{-\lambda_i t}2h_i\left(x_{3i}^Tx_{3i}\right)^{-h_i-1}\left(x_{3i}^Tx_{4i}\right)x_{3i}+e^{-\lambda_i t}\left(x_{3i}^Tx_{3i}\right)^{-h_i}x_{4i} \tag{45}$$

$$\begin{aligned} &k_{1i}>2\delta_i,\ \delta_i>0 \\ &k_{2i}>k_{1i}\frac{5k_{1i}+4\delta_i}{2\,(k_{1i}-2\delta_i)}\delta_i \end{aligned} \tag{46}$$

Proof. We define a Lyapunov function $V_2=\boldsymbol{\xi}^T\boldsymbol{P}\boldsymbol{\xi}$
where

$$\boldsymbol{\xi}=\begin{bmatrix}\xi_1\\ \xi_2\end{bmatrix}=\begin{pmatrix} sign\,(S)\,|S|^{1/2} \\ -k_{2i}\int sign(S)dt\end{pmatrix}$$

$$\boldsymbol{P}=\frac{1}{2}\begin{pmatrix}k_{1i}^2+4k_{2i} & -k_{1i}\\ -k_{1i} & 2\end{pmatrix} \tag{47}$$

Apparently, V_2 is positive definite. Meanwhile, the upper and lower bounds of V_2 can be expressed as

$$\begin{aligned} &\lambda_{\min}(\boldsymbol{P})\,\|\boldsymbol{\xi}\|^2\le V_2\le\lambda_{\max}(\boldsymbol{P})\,\|\boldsymbol{\xi}\|^2 \\ &\|\boldsymbol{\xi}\|^2=|S|+\xi_2^2 \end{aligned} \tag{48}$$

where $\lambda(\bullet)$ represents the eigenvalue of the corresponding matrix.

Taking the derivative of state vector ξ, we get

$$\dot{\boldsymbol{\xi}}=\begin{bmatrix}\frac{1}{2}\dot{S}|S|^{-1/2}\\ -k_{2i}sign(S)\end{bmatrix}=\frac{1}{|S|^{1/2}}\begin{bmatrix}-\frac{1}{2}k_{1i}sign(S)+\frac{1}{2}\xi_2\\ -k_{2i}sign(S)\end{bmatrix}$$

$$=\frac{1}{|S|^{1/2}}\begin{bmatrix}-\frac{1}{2}k_{1i} & \frac{1}{2}\\ -k_{2i} & 0\end{bmatrix}\boldsymbol{\xi}=\frac{1}{|S|^{1/2}}\boldsymbol{A}\boldsymbol{\xi} \tag{49}$$

where

$$\frac{d|S|^{1/2}}{dt}=\frac{1}{2}sign(S)\,\dot{S}|S|^{-1/2} \tag{50}$$

https://doi.org/10.1017/aer.2021.117 Published online by Cambridge University Press

As a result, the derivative of V_2 with respect to t can be obtained

$$\begin{aligned}\dot{V}_2 &= \boldsymbol{\xi}^T \boldsymbol{P}\dot{\boldsymbol{\xi}} + \dot{\boldsymbol{\xi}}^T \boldsymbol{P}\boldsymbol{\xi} \\ &= \boldsymbol{\xi}^T \boldsymbol{P}\frac{1}{|S|^{1/2}}\boldsymbol{A}\boldsymbol{\xi} + \frac{1}{|S|^{1/2}}\boldsymbol{\xi}^T \boldsymbol{A}^T \boldsymbol{P}\boldsymbol{\xi} \\ &= \frac{1}{|S|^{1/2}}\left(\boldsymbol{\xi}^T \boldsymbol{P}\boldsymbol{A}\boldsymbol{\xi} + \boldsymbol{\xi}^T \boldsymbol{A}^T \boldsymbol{P}\boldsymbol{\xi}\right) \\ &= \frac{1}{|S|^{1/2}}\boldsymbol{\xi}^T\left(\boldsymbol{P}\boldsymbol{A} + \boldsymbol{A}^T \boldsymbol{P}\right)\boldsymbol{\xi} \\ &= -\frac{1}{|S|^{1/2}}\boldsymbol{\xi}^T \boldsymbol{Q}\boldsymbol{\xi} \\ &\leq 0\end{aligned} \tag{51}$$

where

$$\boldsymbol{Q} = \frac{1}{2}\begin{bmatrix} k_{1i}^3 + 2k_{1i}k_{2i} & -k_{1i}^2 \\ -k_{1i}^2 & k_{1i} \end{bmatrix} \tag{52}$$

Since matrices $\boldsymbol{P}$, $\boldsymbol{Q}$ and $\boldsymbol{A}$ are constant symmetric positive definite, $\boldsymbol{P}\boldsymbol{A} + \boldsymbol{A}^T\boldsymbol{P} = -\boldsymbol{Q}$ holds based on Equations (51)-(52), which satisfies the Algebraic Lyapunov equation. In turn, this implies that the stability of the dynamics of $\dot{S}$ can be guaranteed in the sense of Lyapunov.

Application of the Rayleigh inequality, yields

$$\dot{V}_2 \leq -\frac{1}{|S|^{1/2}}\boldsymbol{\xi}^T \boldsymbol{Q}\boldsymbol{\xi} \leq -\frac{1}{|S|^{1/2}}\lambda_{\min}(\boldsymbol{Q})\,\|\boldsymbol{\xi}\|^2 \tag{53}$$

Substituting Equation (48) into Equation (53), one can obtain

$$\begin{aligned}\dot{V}_2 &\leq -\frac{1}{|S|^{1/2}}\xi^T \boldsymbol{Q}\boldsymbol{\xi} \leq -\frac{1}{|S|^{1/2}}\lambda_{\min}(\boldsymbol{Q})\,\|\xi\|^2 \\ &\leq -\kappa {V_2}^{1/2}\end{aligned} \tag{54}$$

where $\kappa = \lambda_{\min}^{1/2}(\boldsymbol{P})\,\lambda_{\min}(\boldsymbol{Q})\,/\lambda_{\max}(\boldsymbol{P})$.

Setting $V_2(0) > 0$, gives

$$V_2 = \left(V^{1/2}(0) - \frac{\kappa}{2}t\right) \tag{55}$$

Consequently, $V_2(t)$ can converge to zero in a finite time, and the convergence time can be expressed as

$$T = 2V_2^{1/2}(0)/\kappa \tag{56}$$

On further analysis, based on Equation (41), when the state variables of the system (40) reach the sliding mode surface, one obtains

$$x_{4i} = -\beta_{1i}x_{3i} - \beta_{2i}e^{-\lambda_i t}\left(x_{3i}^T x_{3i}\right)^{-h_4}x_{3i} \tag{57}$$

Then, taking a Lyapunov function V_3

$$V_3 = \frac{1}{2}x_{3i}^2 \tag{58}$$

https://doi.org/10.1017/aer.2021.117 Published online by Cambridge University Press

Table 1. *Initial conditions of missiles*

	Location (km)	Speed (m/s)	Flight path angle (°)
M1	(0,10)	700	5
M2	(0,10)	700	–5
M3	(0,10)	700	2

Thus, the derivative of V_3 can be given by

$$\begin{aligned}\dot{V}_3 &= x_{3i}^T x_{4i} \\ &= x_{3i}^T\left(-\beta_{1i}x_{3i} - \beta_{2i}e^{-\lambda t}\left(x_{3i}^T x_{3i}\right)^{-h_i}x_{3i}\right) \\ &= -\beta_{1i}x_{3i}^T x_{3i} - \beta_{2i}e^{-\lambda_i t}\left(x_{3i}^T x_{3i}\right)^{1-h_i} \\ &= -2\beta_{1i}V_{1i} - 2^{1-h_i}\beta_{2i}e^{-\lambda_i t}V_{1i}^{1-h_i} \\ &\le 0\end{aligned} \tag{59}$$

Finally, by applying lemma 4, all state variables existing in the system (40) will converge to zero in a finite time. Therefore, theorem 2 has been completely proven.

Therefore, the cooperative guidance law with impact angle constraint for intercepting the hypersonic target can be expressed as follows:

$$\begin{cases} u_{Ri} = x_{1i}x_{4i}^2 + \sum_{j=1}^{n} a_{ij}\left[q_{1i}\left(sig\left(x_{1i}-x_{1j}\right)^{\alpha_1}\right) + q_{2i}\left(sig\left(x_{2i}-x_{2j}\right)^{\alpha_2}\left|x_{1i}-x_{1j}\right|^{\alpha_3}\right)\right] \\ u_{qi} = -b_i(x)^{-1}\left(-\dfrac{2x_{2i}x_{4i}}{x_{1i}} + \beta_{1i}x_{4i} + \beta_{2i}A_i\right) - b_i(x)^{-1}\left(k_{1i}|S_i|^{1/2}sign(S_i) + z_i\right) \\ \dot{z}_i = -k_{2i}sign(S_i) \\ A_i = (-\lambda_i)\,e^{-\lambda_i t}\left(x_{3i}^T x_{3i}\right)^{-h_i}x_3 - e^{-\lambda_i t}2h_i\left(x_{3i}^T x_{3i}\right)^{-h_i-1}\left(x_{3i}^T x_{4i}\right)x_{3i} + e^{-\lambda_i t}\left(x_{3i}^T x_{3i}\right)^{-h_i}x_{4i} \end{cases} \tag{60}$$

5.0 Simulation results

In this section, we describe the simulations we have conducted in order to verify the effectiveness and superiority of the guidance law proposed in Equation (60). The simulations included two cases: cooperative interception with different impact angles and cooperative interception with Monte Carlo experiments. In all simulations, it is assumed that three missiles cooperatively intercept a hypersonic target. The target is located at (30km,10km), with a speed of 1800m/s and a target flight path angle of –180°. The gravitational coefficient g = 9.81m/s^2. The initial simulation conditions of the three missiles are shown in Table 1.

For the three-to-one cooperative interception scenario, the communication topology relationship of missiles can be visualised with a graph (see Fig. 3), based on the algebraic graph theory.

The corresponding adjacency matrix of the graph in Fig. 3 can be described as

$$A = \begin{bmatrix} 0 & 1 & 1 \\ 1 & 0 & 1 \\ 1 & 1 & 0 \end{bmatrix}$$

Figure 4 shows the overall cooperative guidance law block diagram. The limitations of the missile guidance commands are $|u_{Ri}| \le 5g$ and $\left|u_{qi}\right| \le 15g$. In order for the simulation to better approximate real conditions, we also take autopilot into consideration, representing by the following first-order lag system

https://doi.org/10.1017/aer.2021.117 Published online by Cambridge University Press

Table 2. *Parameters of the guidance law*

q_{1i}	q_{2i}	α_{1i}	α_{2i}	α_{3i}	h_i
2	2	0.9	0.6	0.33	0.3
β_{1i}	β_{2i}	k_{1i}	k_{2i}	λ_i	
20	0.01	0.2	0.0001	9	

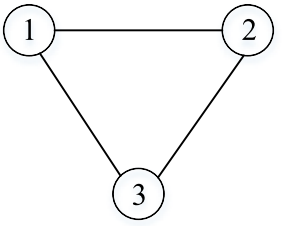

Figure 3. *Communication topology.*

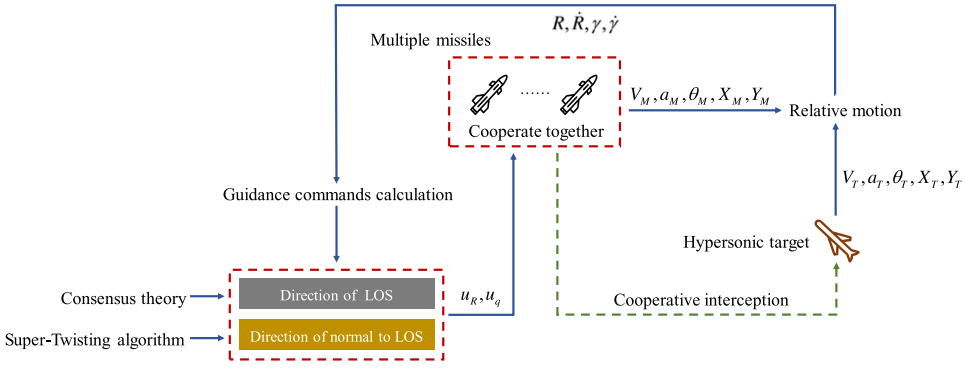

Figure 4. *Overall guidance block diagram.*

$$\frac{u_{aqi}}{u_{qi}} = \frac{u_{aRi}}{u_{Ri}} = \frac{1}{Ts+1} \tag{61}$$

where u_{aqi} and u_{aRi} denote the archived control instructions through the autopilot. Meanwhile, u_{qi} and u_{Ri} are the real control instructions calculated by the guidance law proposed by this paper. The first-order time constant is chosen as $T = 0.3$s.

The corresponding guidance parameters in Equation (60) are given in Table 2.

5.1 Case 1: Cooperative interception with different impact angles

In in order to increase the damage effect on the hypersonic target, we achieved simulation results by setting different constraints on the impact angle. The desired impact angles of the three missiles are 0°, 3°and –3°. In addition, we demonstrated the adaptability of the proposed guidance law in two different scenarios where the target has various manoeuverability. The simulation results are shown in Tables 3 and 4 and Figs. 5 and 6.

For scenario 1, it can be seen from Table 3 that when the target moves at a constant speed, the missiles can intercept the target accurately at the same time with the miss distance of no more than 0.3m.

https://doi.org/10.1017/aer.2021.117 Published online by Cambridge University Press

Table 3. *Analysis of scenario 1 results*

	Scenario 1 $a_T = 0$ m/s^2		
	Miss distance (m)	LOS angle error (°)	Impact time (s)
M1	0.2301	-0.1014×10^{-3}	12.011
M2	0.2300	-0.2114×10^{-3}	12.011
M3	0.2300	-0.2204×10^{-3}	12.011

Table 4. *Analysis of scenario 2 results*

	Scenario 2 $a_T = 20 \sin(\pi t/4 + \pi/4)$ m/s^2		
	Miss distance (m)	LOS angle error (°)	Impact time (s)
M1	0.2784	0.0280	12.026
M2	0.2127	0.0284	12.026
M3	0.3352	0.0269	12.026

And the LOS angle error is extremely small. Figure 5(a) shows the outcome of three missiles launching from the same position, restricted by various constraints of the LOS angle and gradually adjusting their trajectory to intercept the target simultaneously. As seen in Fig. 5(b), the proposed guidance law can guarantee the constraints of impact angle at interception for three missiles, which enables a multi-directional interception mode. The variation range of u_{Ri} for the three missiles change reasonably and smoothly (Fig. 5(c)). At the beginning of terminal guidance, there is a wide fluctuation in the guidance command so as to adjust the posture of the missiles to be consistent. They converge to zero gradually at 8s and maintain course until the interception time. Because of the corresponding constraints of the impact angle, Fig. 5(d) reveals that u_{qi} vary violently at the beginning to ensure IACG, and this does not prevent the desired consistency. Due to the different constraints on impact angle, missiles need to regulate their speed to achieve cooperative interception, in which the total maximum increase is less than 40m/s, a realistic goal (Fig. 5(e)). In Fig. 5(f), the sliding mode surfaces converge to zero rapidly and are smoothly governed by the proposed guidance law, which demonstrates its effectiveness and practicality.

For scenario 2, cooperative interception can be achieved simultaneously with the miss distance no more than 0.4m, which is attainable and acceptable (Table 4). The LOS angle error is less than 0.03°. The proposed guidance law is effective in intercepting a manoeuvering hypersonic target. This and the following findings are illustrated in Fig. 6. The constraints on three missiles' impact angles can be satisfied at interception, which ensures the ability to intercept the target from different directions. For three missiles, the variation in the amplitude of guidance command u_{Ri} varies small and hovers all around zero at the moment of interception. There is a drastic change in the guidance command u_{qi} at the beginning, and then the values become consistent at about 11s till the moment of interception. For a manoeuvering hypersonic target, the three missiles can adjust their speed to satisfy the separate constraints of impact angle and realise cooperative interception. The maximum increase of speed is less than 50m/s, which is reasonable and acceptable. The corresponding sliding mode surface of the three missiles can converge to zero in a finite time and there is no chattering phenomenon during convergence.

5.2 Case 2: Cooperative interception with Monte Carlo experiments

In order to further verify the robustness of the guidance law proposed in this paper, we employ Monte Carlo experiments to assess results in the presence of measurement errors. The initial conditions of the missiles and the target are the same as in scenario 1. In all simulations, it is assumed that the measurement error of $\dot{R}_i$ obeys a Gaussian distribution with a mean value of 0 and a variance of 1m/s, and that the

https://doi.org/10.1017/aer.2021.117 Published online by Cambridge University Press

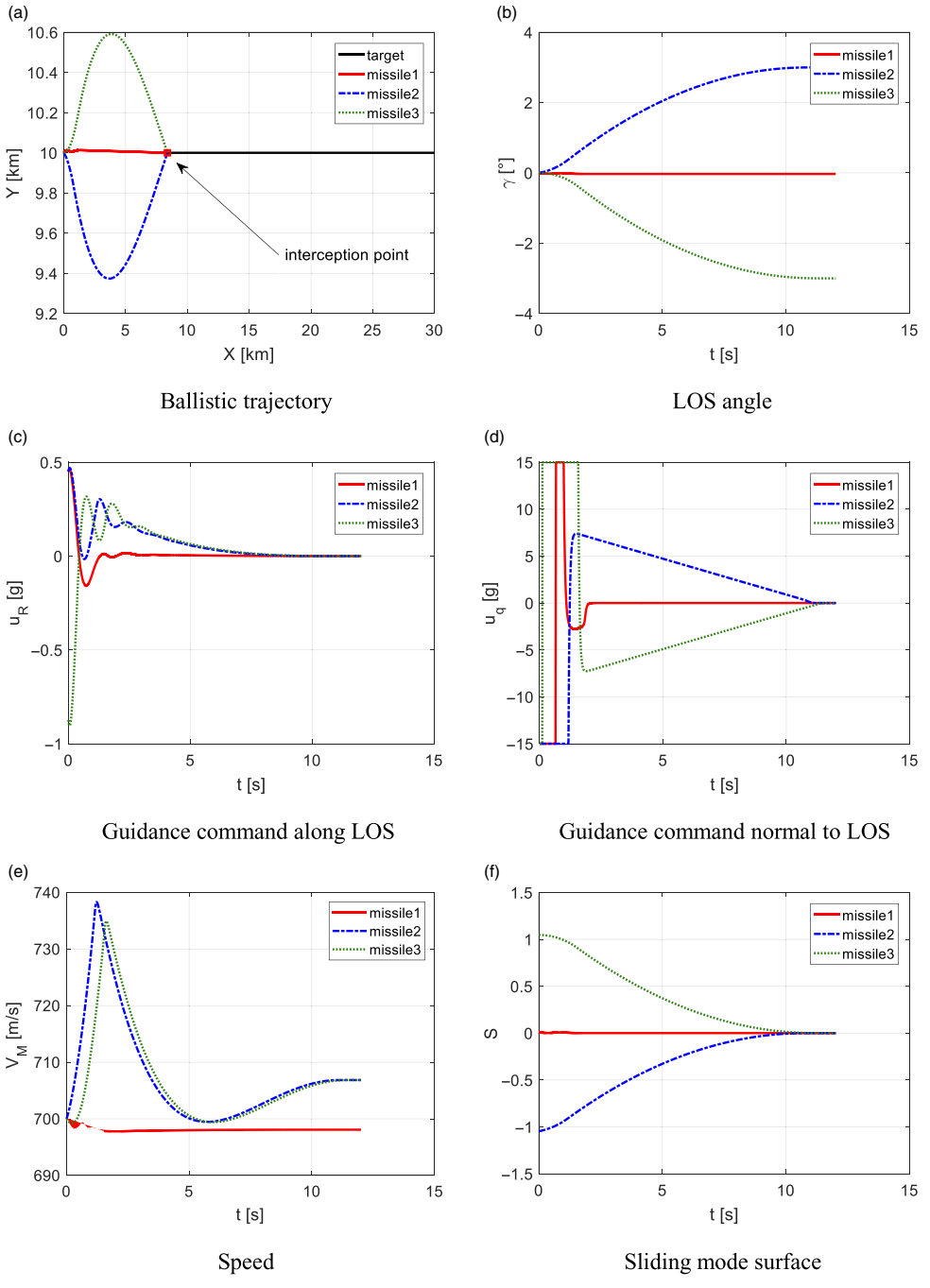

Figure 5. *Simulation results for scenario 1.*

measurement error of $\dot{\gamma}_i$ obeys a Gaussian distribution with a mean value of 0 and a variance of 0.01rad/s. The simulation results are shown in Tables 5 and 6 and Figs. 7 and 8.

The statistical characteristics of miss distance and LOS angle from 300 Monte Carlo simulations demonstrate that the robustness of the guidance law hold up when subjected to the accuracy requirement, although the law is designed to operate under the condition of error noise.

https://doi.org/10.1017/aer.2021.117 Published online by Cambridge University Press

Table 5. *Statistical characteristics of miss distance in Monte Carlo simulations*

	Missile 1	Missile 2	Missile 3
Mean(m)	0.9421	0.9420	0.9418
Variance(m)	0.1996	0.1996	0.2163

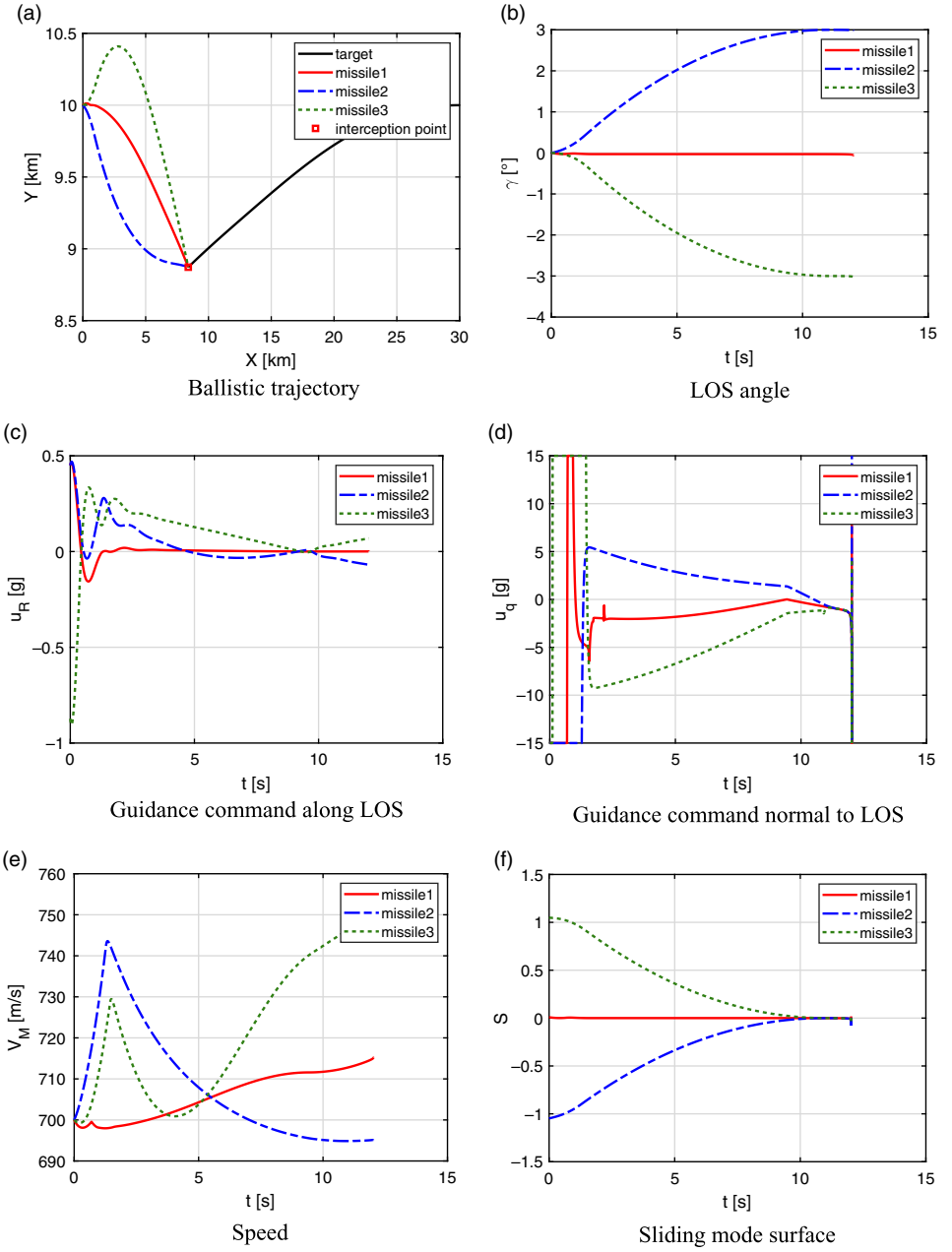

Figure 6. *Simulation results for scenario 2.*

https://doi.org/10.1017/aer.2021.117 Published online by Cambridge University Press

Table 6. *Statistical characteristics of LOS angle in Monte Carlo simulations*

Parameter	Missile 1	Missile 2	Missile 3
Mean(°)	–0.0337	2.9954	–3.0039
Variance(°)	7.9138×10^{-6}	9.4295×10^{-6}	6.8179×10^{-6}

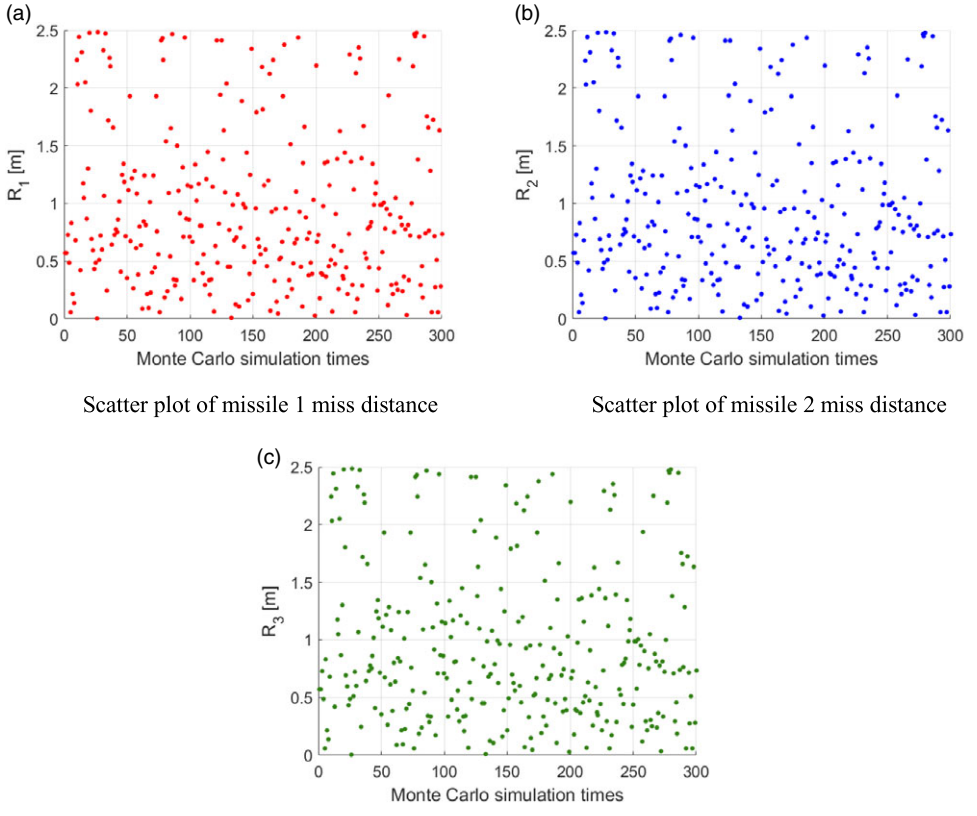

Scatter plot of missile 1 miss distance

Scatter plot of missile 2 miss distance

Scatter plot of missile 3 miss distance

Figure 7. *Monte Carlo simulation results for miss distance.*

6.0 Conclusions

Based on the premise of multiple inferior missiles cooperatively intercepting a hypersonic target, we conduct systematic and intensive research based on consensus theory, homogeneous system theory, and sliding mode control theory. The principal results obtained are as follows:

1. A cooperative guidance law that takes variation of missile speed into consideration can improve missile manoeuverability. For a uniform moving target, the total maximum increase is less than 40m/s, and for a manoeuvering target, the total maximum increase is no more than 50m/s, which is satisfactory.
2. Aiming at the unknown target acceleration information, based on NFTSM sliding mode surface, the guidance command for normal to LOS designed with the super-twisting algorithm, which improves the practical application value.
3. The proposed guidance law can not only intercept the target accurately but also at the desired impact angle, thus improving target damage efficiency.

https://doi.org/10.1017/aer.2021.117 Published online by Cambridge University Press

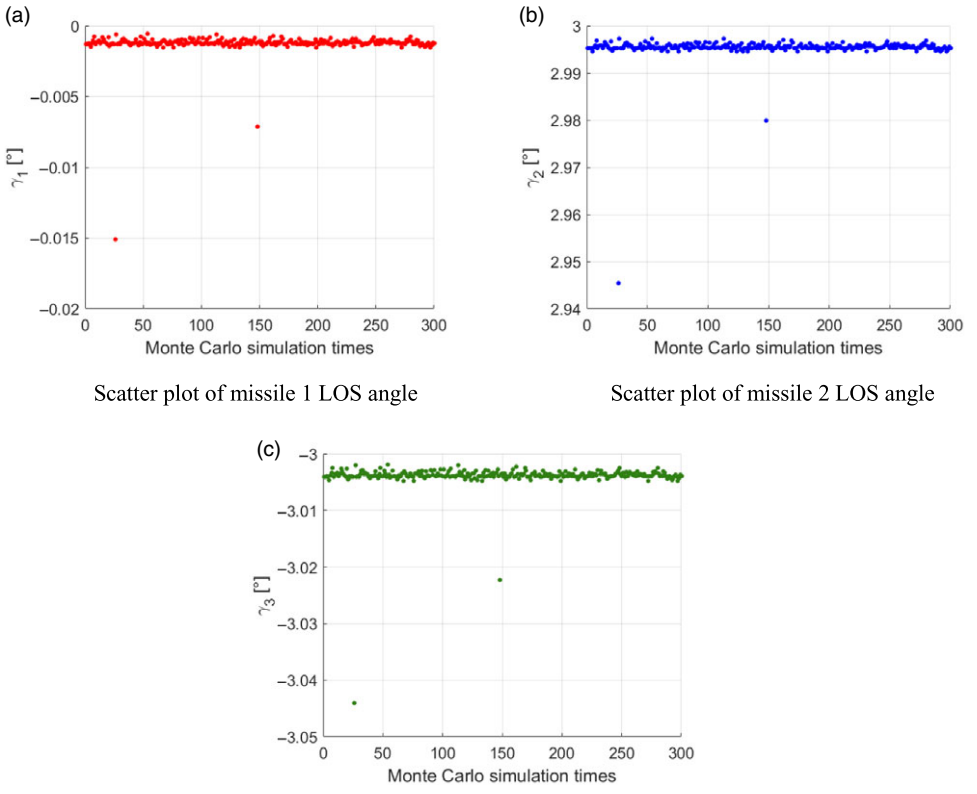

Scatter plot of missile 1 LOS angle

Scatter plot of missile 2 LOS angle

Scatter plot of missile 3 LOS angle

Figure 8. *Monte Carlo simulation results for LOS angle.*

It is evident that these findings warrant further investigation of the interception of hypersonic targets. However, it is worth making future research on the design of cooperative guidance law with time-varying communication topology in the three-dimensional plane.

Acknowledgments. The authors would like to appreciate the support from the National Natural Science Foundation of China (NSFC) (61603297), the Natural Science Foundation of Shaanxi Province (2020JQ-219) and the Shanghai Aerospace Science and Technology Innovation Fund (SAST2020-004). Besides, the authors gratefully show much gratitude to the reviewers for their careful work and thoughtful suggestions that have helped improve this paper substantially.

Declaration of competing interest. All the authors declare that they have no known competing financial interests or personal relationships that could have appeared to influence the work reported in this paper.

References

[1] Bolender, M.A. (2009, June). An overview on dynamics and controls modelling of hypersonic vehicles. In 2009 American control conference (pp. 2507–2512). IEEE.

[2] An, H., Wu, Q., Wang, G., Guo, Z. and Wang, C. Simplified longitudinal control of air-breathing hypersonic vehicles with hybrid actuators. *Aerosp. Sci. Technol.*, 2020, **104**, pp 105936.

[3] Zhao, Z.T., Huang, W., Yan, L. and Yang, Y.G. An overview of research on wide-speed range waverider configuration. *Prog. Aerosp. Sci.*, 2020, **113**, pp 100606.

[4] Yan, B., Dai, P., Liu, R., Xing, M. and Liu, S. Adaptive super-twisting sliding mode control of variable sweep morphing aircraft. *Aerosp. Sci. Technol.*, 2019, **92**, pp 198–210.

[5] Zhao, Z.T., Huang, W., Yan, B.B., Yan, L., Zhang, T.T. and Moradi, R. Design and high speed aerodynamic performance analysis of vortex lift waverider with a wide-speed range. *Acta Astronautica*, 2018, **151**, pp 848–863.

[6] Dai, P., Yan, B., Huang, W., Zhen, Y., Wang, M. and Liu, S. Design and aerodynamic performance analysis of a variable-sweep-wing morphing waverider. *Aerosp. Sci. Technol.*, 2020, **98**, pp 105703.

https://doi.org/10.1017/aer.2021.117 Published online by Cambridge University Press

[7] Leng, J.X., Shen, Y., Zhang, T.T., Huang, W. and Yan, L. Parameterized modeling and optimization of reusable launch vehicles based on reverse design approach. *Acta Astronautica*, 2020, **178**, pp 36–50.
[8] Xu, B. and Shi, Z. An overview on flight dynamics and control approaches for hypersonic vehicles. *Sci. China Inf. Sci.*, 2015, **58**, (7), pp 1–19.
[9] Shiyu, Z. and Rui, Z. Cooperative guidance for multimissile salvo attack. *Chinese J. Aeronaut.*, 2008, **21**, (6), pp 533–539.
[10] Zhao, Q., Dong, X., Liang, Z. and Ren, Z. Distributed group cooperative guidance for multiple missiles with fixed and switching directed communication topologies. *Nonlinear Dyn.*, 2017, **90**, (4), pp 2507–2523.
[11] Nikusokhan, M. and Nobahari, H. Closed-form optimal cooperative guidance law against random step maneuver. *IEEE Trans. Aerosp. Electron. Syst.*, 2016, **52**, (1), pp 319–336.
[12] Zhang, Y., Ma, G. and Liu, A. Guidance law with impact time and impact angle constraints. *Chinese J. Aeronaut.*, 2013, **26**, (4), pp 960–966.
[13] Sinha, A. and Kumar, S.R. Supertwisting Control-Based Cooperative Salvo Guidance Using Leader–Follower Approach. *IEEE Trans. Aerosp. Electron. Syst.*, 2020, **56**, (5), pp 3556–3565.
[14] Zhang, C., Song, J., & Huang, L. (2017, July). The time-to-go consensus of multi-missiles with communication delay. In 2017 36th Chinese Control Conference (CCC) (pp. 7634–7638). IEEE.
[15] Chen, Y., Wang, J., Wang, C., Shan, J. and Xin, M. A modified cooperative proportional navigation guidance law. *J. Franklin Inst.*, 2019, **356**, (11), pp 5692–5705.
[16] Yan, P., Fan, Y., Liu, R. and Wang, M. Distributed target-encirclement guidance law for cooperative attack of multiple missiles. *Int. J. Adv. Robot. Syst.*, 2020, **17**, (3).
[17] Jeon, I.S., Lee, J.I. and Tahk, M.J. Impact-time-control guidance law for anti-ship missiles. *IEEE Trans. Control Syst. Technol.*, 2006, **14**, (2), pp 260–266.
[18] Zhou, J. and Yang, J. Distributed guidance law design for cooperative simultaneous attacks with multiple missiles. *J. Guid. Control Dyn.*, 2016, **39**, (10), pp 2439–2447.
[19] Biao, Y.A.N.G., Wuxing, J.I.N.G. and Changsheng, G.A.O. Three-dimensional cooperative guidance law for multiple missiles with impact angle constraint. *J. Syst. Eng. Electron.*, 2020, **31**, (6), pp 1286–1296.
[20] Zhang, W., Du, X. and Xia, Q. A Three-Dimensional Cooperative Guidance Law Based on Consensus Theory for Maneuvering Targets. *Math. Probl. Eng.*, 2019, 2019.
[21] Huang, J., Zhang, Y. and Liu, Y. A biased proportional guidance algorithm for moving target with impact angle and field-of-view constraints. *J. Astronaut.*, 2016, **37**, (2), pp 195–202.
[22] You, H. and Zhao, F.J. Distributed synergetic guidance law for multiple missiles with angle-of-attack constraint. *Aeronaut. J.*, 2020, **124**, (1274), pp 533–548.
[23] Kumar, S.R., Rao, S. and Ghose, D. Sliding-mode guidance and control for all-aspect interceptors with terminal angle constraints. *J. Guid. Control Dyn.*, 2012, **35**, (4), pp 1230–1246.
[24] Zhou, J., Wang, Y. and Zhao, B. Impact-time-control guidance law for missile with time-varying velocity. *Math. Probl. Eng.*, 2016, 2016.
[25] Ma, S., Wang, X. and Wang, Z. Impact Time Control Guidance Law for Guided Projectile Considering Time-Varying Velocity. 2019 SICE International Symposium on Control Systems (SICE ISCS), 2019.
[26] Li, B., Lin, D., Wang, J. and Tian, S. Guidance law to control impact angle and time based on optimality of error dynamics. *Proc. Inst. Mech. Eng. G J. Aerosp. Eng.*, 2019, **233**, (10), pp 3577–3588.
[27] Ren, W. and Cao, Y. *Distributed coordination of multi-agent networks: emergent problems, models, and issues*, Springer Science & Business Media, 2010
[28] Olfati-Saber, R. and Murray, R.M. Consensus problems in networks of agents with switching topology and time-delays. *IEEE Trans. Automat. Control*, 2004, **49**, (9), pp 1520–1533.
[29] Mei, J., Ren, W. and Ma, G. Distributed coordination for second-order multi-agent systems with nonlinear dynamics using only relative position measurements. *Automatica*, 2013, **49**, (5), pp 1419–1427.
[30] Hong, Y., Xu, Y. and Huang, J. Finite-time control for robot manipulators. *Syst. Control Lett.*, 2002, **46**, (4), pp 243–253.
[31] Wang, X. and Hong, Y. Finite-time consensus for multi-agent networks with second-order agent dynamics. *IFAC Proc. volumes*, 2008, **41**, (2), pp 15185–15190.
[32] Rosier, L. Homogeneous Lyapunov function for homogeneous continuous vector field. *Syst. Control Lett.*, 1992, **19**, (6), pp 467–473.
[33] Bhat, S.P. and Bernstein, D.S. Continuous finite-time stabilization of the translational and rotational double integrators. *IEEE Trans. Automat. Control*, 1998, **43**, (5), pp 678–682.
[34] Wang, J., Zhao, Z. and Zheng, Y. NFTSM-based Fault Tolerant Control for Quadrotor Unmanned Aerial Vehicle with Finite-Time Convergence. *IFAC-PapersOnLine*, 2018, **51**, (24), pp 441–446.
[35] Vazquez, C., Collado, J. and Fridman, L. Super twisting control of a parametrically excited overhead crane. *J. Franklin Inst.*, 2014, **351**, (4), pp 2283–2298.
[36] Chalanga, A., Kamal, S., Fridman, L.M., Bandyopadhyay, B. and Moreno, J.A. Implementation of super-twisting control: Super-twisting and higher order sliding-mode observer-based approaches. *IEEE Trans. Ind. Electron.*, 2016, **63**, (6), pp 3677–3685.
[37] Bhat, S.P. and Bernstein, D.S. Finite-time stability of continuous autonomous systems. *SIAM J. Control Optim.*, 2000, **38**, (3), pp 751–766.

Cite this article: Liu S., Yan B., Liu R., Dai P., Yan J. and Xin G. (2022). Cooperative guidance law for intercepting a hypersonic target with impact angle constraint. *The Aeronautical Journal*, **126**, 1026–1044. https://doi.org/10.1017/aer.2021.117